Supporting Information

Observation of Radical Rebound in a Mononuclear Nonheme Iron Model Complex

Thomas M. Pangia,[†] Casey G. Davies,[‡] Joshua R. Prendergast,[‡,§] Jesse B. Gordon,[†] Maxime A. Siegler,[†] Guy N. L. Jameson,*[,‡,§] and David P. Goldberg*[,†]

[†]Department of Chemistry, The Johns Hopkins University, 3400 North Charles Street, Baltimore, Maryland, 21218, USA

‡Department of Chemistry and MacDiarmid Institute for Advanced Materials and Nanotechnology, University of Otago, P.O. Box 56, Dunedin 9054, New Zealand

[§]School of Chemistry, Bio21 Molecular Science and Biotechnology Institute, The University of Melbourne, 30 Flemington Road, Parkville, Victoria 3010, Australia

Contents

I. General Methods and Materials. All chemicals and reagents were purchased from Sigma-Aldrich, Fisher Scientific, Acros Organics, Merck, Fluka Analytical, or Alfa Aesar and were used without further purification unless noted otherwise. Solvents (methanol, diethyl ether, acetonitrile, and tetrahydrofuran) used in organic synthesis were purified via Pure-Solv Solvent Purification System from Innovative Technology, Inc. Carbon tetrachloride was purchased from Fisher Scientific and used without further purification. For Mössbauer spectroscopy, ^{57}Fe (95.93% isotope-enriched) was purchased from Cambridge Isotope Laboratories. Solvents used in the reactions of the iron(II) and iron(III) complexes were subjected to additional purification after initial purification via a Pure-Solv Solvent Purification System. Acetonitrile was distilled over calcium hydride. THF was distilled from sodium/benzophenone. All solvents were degassed by freeze-pump-thaw cycles and stored in a N_2 filled dry box. Reactions involving inert atmosphere were performed using either standard Schlenk techniques or in a dry box. The compounds 1,1-bis(6-phenylpyridin-2-yl)-*N*-(pyridin-2-ylmethyl)methanamine,[1] 2-(bromomethyl)phenyl acetate,[2] and Gomberg's Dimer (1,1',1"-(((4-(diphenylmethylene)-2,5-cyclohexadien-1-yl)methylidyne)trisbenzene, $(Ph_3C)_2$)[3-5] were prepared according to literature procedures. $^{57}Fe(ClO_4)_2$ was synthesized by reaction of perchloric acid with ^{57}Fe in distilled, degassed acetonitrile under airfree conditions, forming a solution which was used without further purification. *Caution: Perchlorate salts of metal complexes are potentially explosive. Care should be taken when handling these compounds*. *Note: trityl radical is O_2 and light-sensitive. Measures should be taken to avoid exposure of the radical to light and air.*

II. Analytical Methods. Kinetic UV-vis measurements were performed on a Hewlett-Packard Agilent 8453 diode-array spectrophotometer with a 3.5 mL quartz cuvette (path length = 1 cm) equipped with a septum. Other UV-visible spectra were recorded on a Varian Cary 50 Bio spectrophotometer. NMR spectra were collected on a Bruker Avance 400 MHz FT-NMR spectrometer. Electron paramagnetic resonance (EPR) spectra were obtained on a Bruker EMX EPR spectrometer controlled with a Bruker ER 041 X G microwave bridge. The EPR spectrometer was equipped with a continuous-flow liquid He cryostat and an ITC503 temperature controller made by Oxford Instruments, Inc. Elemental analyses on air-stable compounds were performed by Atlantic Microlab Inc., Norcross, GA. Elemental analyses on air-sensitive compounds were performed by Midwest Microlabs, Indianapolis, IN. Gas Chromatography (GC-FID) was carried

out on an Agilent 6890 gas chromatograph fitted with a DB–5 5% phenylmethyl siloxane capillary column (30 m x 0.32 mm x 0.25 µm) and equipped with a flame–ionization detector. FAB-MS was obtained using a VG analytical VG-70SE magnetic sector mass spectrometer. Mössbauer spectroscopy was performed on a spectrometer from SEE Co. (Science Engineering & Education Co., MN) equipped with a closed cycle refrigerator system from Janis Research Co. and SHI (Sumitomo Heavy Industries Ltd.) Spectra were measured with a small magnetic field (47 mT) applied parallel to the gamma radiation. Fitted parameters are presented in Table S1.

III. Synthesis.

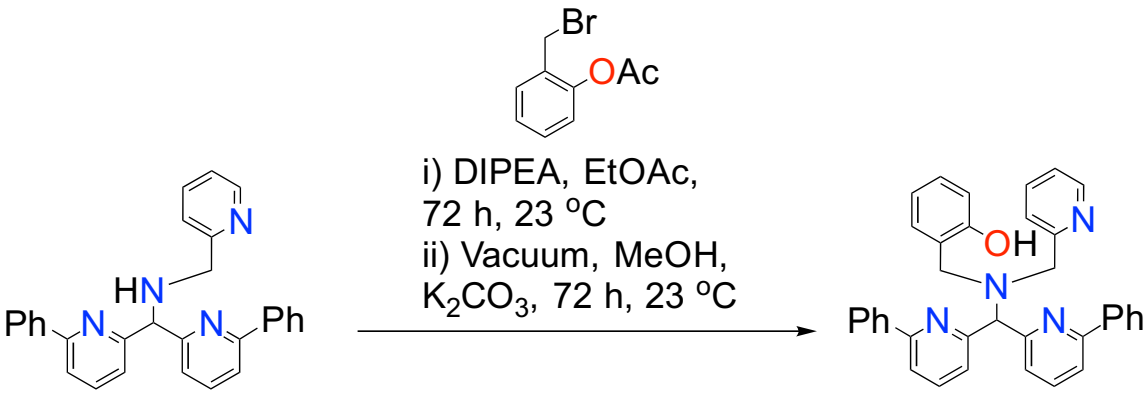

Scheme S1. Synthesis of N3Py^{2Ph}OH.

Synthesis of 2-(((bis(6-phenylpyridin-2-yl)methyl)(pyridin-2-ylmethyl)amino)methyl)phenol (N3Py^{2Ph}OH). The synthesis was adapted from a previous literature procedure.[6] An amount of 1,1-bis(6-phenylpyridin-2-yl)-*N*-(pyridin-2-ylmethyl)methanamine (1.21 g, 2.82 mmol) was dissolved in ethyl acetate (20 mL) in a 100 mL round bottom flask (Scheme S1). An amount of 2-(bromomethyl)phenyl acetate (0.77 g, 3.37 mmol) was dissolved in ethyl acetate (10 mL) and added to the amine solution, followed by addition of diisopropylethylamine (1.0 mL, 5.9 mmol). The reaction was stirred for 72 h at 23 °C. The organic solvent was removed under vacuum, and methanol (30 mL) was added, followed by potassium carbonate (2.21 g, 16 mmol) and stirring for 72 h at 23 °C. The resulting slurry was filtered through Celite and the filtrate concentrated under vacuum. The crude product was purified by column chromatography on silica gel with CH_2Cl_2/MeOH gradient as eluent. The compound was obtained as a yellow solid (0.518 g, 34%). ^{1}H NMR ($CDCl_3$): δ 11.31-11.20 (br s, 1H), 8.74-8.60 (m, 1H), 8.10-8.01 (m, 4H), 7.79-7.65 (m, 4H), 7.64-7.56 (m, 1H), 7.53-7.33 (m, 9H), 7.24-7.14 (m, 2H), 7.13-7.07 (m, 1H), 6.96-6.87 (m,

1H), 6.82-6.75 (m, 1H), 5.56-5.50 (s, 1H), 4.25-4.17 (s, 2H), 4.11-4.03 (s, 2H). ^{13}C NMR ($CDCl_3$): δ 159.0, 158.9, 158.0, 156.5, 148.7, 139.4, 137.0, 136.8, 130.6, 128.9, 128.8, 128.7, 127.1, 123.6, 123.0, 122.8, 122.2, 118.9, 118.7, 116.6, 69.6, 56.3, 54.6. FAB-MS: *calcd* for $[M+H]^+$ 535.2498, observed mass: 535.2486.

Synthesis of [Fe^{II}(N3PyO^{2Ph})(CH_3CN)](ClO_4) (1). Under an inert atmosphere, N3Py^{2Ph}OH (40 mg, 0.07 mmol) was dissolved in 5 mL of acetonitrile, to which was added triethylamine (10 μL, 0.07 mmol). The reaction mixture was stirred for 5 min. To this solution was added $Fe(ClO_4)_2$•xH_2O (18 mg, 0.07 mmol), resulting in an instant change from yellow to dark brown. The solvent was removed in vacuo and the brown residue redissolved in methanol (2 mL) and filtered through Celite. Vapor diffusion of diethyl ether gave red-brown crystalline prisms of **1** after 1-2 weeks (15 mg, 27%) suitable for X-ray diffraction (Figure S1). ^{1}H NMR (CD_3CN): δ 72.6, 61.5, 51.2, 49.4, 45.5, 36.1, 31.8, 25.3, 19.2, 15.1, -8.2, -24.1, -27.3 (Figure S10). *Anal. Calcd* for ($C_{38}H_{32}ClFeN_5O_5$)•(CH_3OH)•0.5(CH_3CN): C, 61.47, H; 4.76; N, 9.19. Found: C, 60.48; H, 4.65; N, 8.76. UV-Vis (CH_3CN) (23 °C): Slight shoulder, λ = 450 nm (ε = 900 M^{-1} cm^{-1}). Figure S2.

Synthesis of [Fe^{III}(N3PyO^{2Ph})(OCH_3)](ClO_4) (2). Under an inert atmosphere, a solution of **1** was generated in situ following the above procedure (0.05 mmol scale). Following filtration through Celite, the resulting solution of **1** was placed under vacuum to remove the organic solvent. The remaining brown residue was dissolved in 5 mL methanol and filtered through Celite an additional time. The brown methanol solution was removed from the inert atmosphere and exposed to air for 8 h, forming a purple solution (Figure S4, S5). The purple solution was concentrated under vacuum and redissolved in methanol (1 mL). Vapor diffusion of diethyl ether formed dark purple crystalline rods of **2** after 2 days (17 mg, 41%) suitable for X-ray diffraction (Figure S3). ^{1}H NMR (THF-d_8): δ 88.2, 72.0, 63.0, 60.0, 55.4, 51.3, 48.3, 39.4, 38.6, 28.2, 27.0, 25.5, 16.6, -9.5, -15.5,-20.9 (Figure S11). *Anal. Calcd* for ($C_{37}H_{32}ClFeN_4O_6$)•(H_2O)•0.4($C_4H_{10}O$): C, 60.89, H; 4.93; N, 7.21. Found: C, 60.70; H, 4.74; N, 8.08. UV-vis (CH_3OH) (room temperature): λ = 550 nm (ε = 1290 M^{-1} cm^{-1}) (Figure S4). EPR (THF, 13 K): g = 4.26 (Figure S6). Subsequent reactions were performed with either crystalline material or **2** generated in situ. In absence of crystalline material,

an amount of **2** was generated by reacting $N3Py^{2Ph}OH$ with equimolar amounts of Et_3N and $Fe(ClO_4)_2$ in acetonitrile in an inert atmosphere. Following filtration, the acetonitrile was removed under reduced pressure and the resulting residue redissolved in methanol. Exposure to air brought about the formation of **2**, which was isolated by evaporation of methanol. ^{1}H NMR spectra of **2** generated *in situ* matches that seen for crystalline **2** dissolved in THF-d_8. No difference in reactivity between trityl radical and **2** prepared by either method was observed.

IV. Experimental Details.

$[Fe^{II}(N3PyO^{2Ph})(CH_3CN)](ClO_4)$ (1). Mössbauer Spectroscopy. A solution of ^{57}Fe enriched **1** (4 mM) in THF was produced anaerobically in a glove box and frozen in a Mössbauer cup. The Mössbauer spectrum was collected at 5.2 K (Figure S16).

Reaction of 2 with Gomberg's dimer. UV-vis Spectroscopy. A solution of **2** (3 mL, 0.5 mM) in THF was placed in a quartz cuvette (1 cm pathlength) under inert atmosphere. The solution was heated to 50 °C and an initial spectrum recorded. Gomberg's dimer, $(Ph_3C)_2$, (1.6 equiv in 0.1 mL THF) was added and the UV-vis bands at λ_{max} = 516 nm (triphenyl methyl radical in THF) and λ_{max} = 570 nm (**2** in THF) were monitored over 1 h. Decay (~80%) of the peak at 570 nm was observed over the time period, denoting the consumption of the Fe^{III} starting material (Figure S7). Heating **2** in THF over 1 h with no $(Ph_3C)_2$ produces a slow background decomposition when monitored by UV-vis, accounting for ~25% loss of **2** (Figure S8).

Reaction of 2 with $(Ph_3C)_2$. EPR Spectroscopy. A solution of **2** (2 mM) in THF was heated to 50 °C. An amount of $(Ph_3C)_2$ (1.6 equiv) was added. Aliquots (0.5 mL) were removed at the following time points: 0 min, 1 min, 5 min, 30 min, and 60 min and placed in separate 4 mm inner diameter quartz EPR tubes and frozen in liquid nitrogen. Each aliquot was then analyzed by X-band EPR at 13 K. A decrease in the signal at g = 4.26 was observed over time, consistent with consumption of **2** and formation of an EPR-silent Fe^{II} species equivalent to **1** (Figure S9).

Reaction of 2 with $(Ph_3C)_2$. ^{1}H NMR Spectroscopy. A solution of **2** (0.6 mL, 3.5 mM) in THF-d_8 was heated to 50 °C in a sealed NMR tube and an initial spectrum was recorded. An amount of $(Ph_3C)_2$ (4 equiv) was added and the solution manually mixed in the NMR tube. A spectrum

recorded after 60 min at 50 °C showed formation of a peak at 3.04 ppm matching the –OCH_3 signal of Ph_3COCH_3, the expected rebound product. Integration against an internal standard (Ph-C_6H_4-OCH_3, 3.2 mM) gave a yield of 60% for Ph_3COCH_3 (based on **2**, Figure S13). The paramagnetic spectrum of **2** with peaks between +100 to -40 ppm disappeared after 60 min and a new spectrum with peaks between +90 and -40 ppm was observed. Removal of the reaction solvent and dissolution of the brown residue in CD_3CN resulted in a spectrum that could be assigned to **1** (Figures S10, S11, S14). Control experiments between $(Ph_3C)_2$ and sodium methoxide (10 equiv and 100 equiv) produced no detectable Ph_3COCH_3. Control experiments between $(Ph_3C)_2$ and methanol (10 equiv and 100 equiv) also did not produce Ph_3COCH_3.

Reaction of 2 with $(Ph_3C)_2$. Gas Chromatography. A solution of **2** in THF (4 mM, 1 mL) was combined with $(Ph_3C)_2$ (3 equiv) and the internal standard Ph-C_6H_4-OCH_3 (2.2 mM). The solution was heated for 60 min at 50 °C. An aliquot (100 μL) was combined with 100 μL of oxygenated THF to quench the reaction. The resulting solution was injected (2 μL) onto the GC-FID. The Ph_3COCH_3 (R_T = 12.4 min) was quantified from a calibration curve with the Ph-C_6H_4-OCH_3 internal standard (R_T = 8.1 min) (Figure S15). Each reaction was injected twice, obtaining an average yield of 58%.

Reaction of 2 with $(Ph_3C)_2$. Mössbauer Spectroscopy. A solution of **2-^{57}Fe** was made in THF in a glove box under an inert atmosphere (N_2(g)). To the resulting dark purple solution was added 1.6 equiv $(Ph_3C)_2$ dissolved in THF. Equal volumes of each solution, preheated to 50 ^{o}C, were added to give final concentrations of 4 mM of **2-^{57}Fe** and 6.4 mM of $(Ph_3C)_2$. The reaction was kept at 50 ± 1 ^{o}C in a water bath. The dark purple solution rapidly turned light yellow-brown and was incubated for a total of 70 min. The reaction mixture was then frozen anaerobically at 77 K in a Mössbauer cup and stored until spectra could be collected (Table S1). Mössbauer spectra of **2-^{57}Fe** and the final reaction mixture were recorded (Figure S16). Additional measurements of a solid-phase crystalline sample of **2** (35 mg in boron-nitride) were made at 100 K for comparison with solution-phase samples (Figure S17, Table S1).

Evans method measurement of the solution magnetic moment of 2. A stock solution of toluene in THF-d_8 (9% toluene) was prepared by mixing toluene (50 μL) into THF-d_8 (500 μL). A 75 μL

aliquot was injected into a glass capillary which was flame sealed and inserted into an NMR tube. A solution of **2** (1.4 mM) was prepared in THF-d_8 (500 μL)/ toluene (50 μL), then transferred to the NMR tube containing the sealed capillary tube, and an ^{1}H NMR spectrum was recorded (Figure S18). The chemical shift of the singlet assigned to the -CH_3 peak for toluene in the presence of the paramagnetic complex was compared with that of the same peak in the inserted capillary tube. The effective spin-only magnetic moment was calculated by simplified Evans method[7-8] using the equation $\mu_{eff} = 0.0618(\Delta\nu T/2fM)^{1/2}$, where f is the oscillator frequency (MHz) of the superconducting spectrometer, T is temperature (K), M is the molar concentration of the paramagnetic metal complex, and $\Delta\nu$ is the frequency difference (Hz) between the two reference toluene -CH_3 signals. The data shown in Figure S18 gave $\Delta\nu = 28.01$ Hz, $\mu_{eff} = 5.3\ \mu_B$, which is close to the calculated spin-only value for high-spin Fe^{III} (d^5), $\mu_{eff} = 5.9\ \mu_B$.

DFT Computational Studies.

All calculations were performed in the *ORCA-3.0.2* program package.[9] Initial geometries were obtained from X-ray crystallographic models. Optimized geometries were calculated using the BP86 functional.[10-11] Geometries were also calculated using the TPSSh functional,[12-13] which yielded similar geometries to those with BP86. The 6-311g* basis set was used for all Fe, N, O, and Cl atoms and the 6-31g* basis set was for all C and H atoms. A continuum solvation model was included (COSMO) with acetonitrile used for **1-MeCN** and **2**, and THF for **1-THF** and **1-5C**. Due to SCF convergence difficulties in **1-MeCN** damping parameters were altered using the Slowconv function in ORCA. Frequency calculations at the same level of theory confirmed that all optimizations had converged to true minima on the potential energy surface (i.e., no imaginary frequencies). The optimized structures using the BP86 functional were used for Mössbauer calculations for **1-MeCN**, **1-THF**, and **1-5C** because of the close match between the X-ray crystallographic and calculated metrics for **1-MeCN**. However, we were unable to obtain a geometry optimization of **2** using BP86 and instead employed the TPSSh functional. Mössbauer parameters were computed using the B3LYP[14-17] functional and the def2-TZVP[18-19] basis set for all atoms, or a combination of CP(PPP)[20] for Fe and def2-TZVP for all other atoms. The angular integration grid was set to Grid4 (NoFinalGrid), with increased radial accuracy for the Fe atom (IntAcc 7). To simulate solid state effects, a continuum solvation model was included (COSMO) with a solvent of intermediate dielectric (methanol).The isomer shift was obtained from the

electron density at the Fe nucleus, using a linear fit function previously reported: $\delta = \alpha(\rho(0) - c) + \beta$.[21] For the methodology described here, $\alpha = -0.424$ au^3 mm s^{-1}, $\beta = 7.55$ mm s^{-1}, and $c = 11800$ au^{-3}.

V. Single Crystal X-Ray crystallography. All reflection intensities were measured at 110(2) K using a SuperNova diffractometer (equipped with Atlas detector) with Mo $K\alpha$ radiation (λ = 0.71073 Å) for **1** or with Cu $K\alpha$ radiation (λ = 1.54178 Å) for **2** under the program CrysAlisPro (Version 1.171.36.32 Agilent Technologies, 2013). The same program was used to refine the cell dimensions and for data reduction. Both structures were solved with the program SHELXS-2014 (Sheldrick, 2008) and were refined on F^2 with SHELXL-2014 (Sheldrick, 2008).[22] Analytical numeric absorption correction based on a multifaceted crystal model was applied using CrysAlisPro. The temperature of the data collection was controlled using the system Cryojet (manufactured by Oxford Instruments). The H atoms were placed at calculated positions using the instructions AFIX 13, AFIX 23, AFIX 43, AFIX 137 or AFIX 147 with isotropic displacement parameters having values 1.2 *U*eq or 1.5 of the attached C or O atoms. For **2**, the H atoms attached to O1W/O1W' (disordered lattice water molecule) could not be retrieved from difference Fourier maps.

Crystal Structure of 1. The ClO_4^- counterion is found to be disordered over two orientations, and the occupancy factor of the major component refines to 0.780(7). The asymmetric unit also contains one site occupied with a disordered mixture of solvent molecules (MeOH with occupancy factor of 0.618(2) and MeCN with occupancy factor of 0.382(2)).

1, Fw = 765.47, orange block, 0.41 × 0.35 × 0.22 mm^3, monoclinic, $P2_1/n$, a = 10.1120(3), b = 22.0629(6), c = 16.4935(4) Å. α = 90, β = 104.954(3), γ = 90°, V = 3555.08(17) $Å^3$, Z = 4, μ = 0.56 mm^{-1}, abs. corr. range: 0.838-0.915. 28564 Reflections were measured up to a resolution of $(\sin\theta/\lambda)_{max}$ = 0.650 $Å^{-1}$. 8157 Reflections were unique (R_{int} = 0.0244), of which 7099 were observed [$I > 2\sigma(I)$]. 542 Parameters were refined with 123 restraints. R1/wR2 [I >2σ(I)]: 0.0361/0.0884. *R*1/*wR*2 [all refl.]: 0.0436/0.0927. S = 1.04. Residual electron density found between -0.32 and 0.52 e $Å^{-3}$.

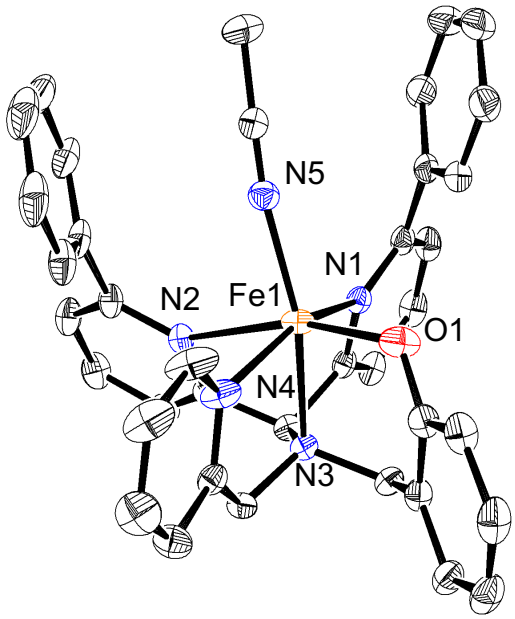

Figure S1. Displacement ellipsoid plot (50% probability level) of the cation of **1**. H atoms, lattice solvent molecules, and ClO_4^- counterion have been omitted for clarity. Selected bond distances (Å) and angles (°): Fe1-N1 2.2633(13), Fe1-N2 2.473(3), Fe1-N3 2.1699(13), Fe1-N4 2.1598(14), Fe1-O1 1.9560(13), Fe1-N5 2.0769(14), N3-Fe1-N5 163.95(5), N1-Fe1-N4 155.78(5), O1-Fe1-N2 164.43(5), N5-Fe1-N4 101.54(5), N4-Fe1-N3, 79.02(5), O1-Fe1-N1 99.71(5), N4-Fe1-N2 85.40(5), N2-Fe1-N1 80.41(5), N4-Fe1-O1 88.82(6), N5-Fe1-O1 103.96(6), N5-Fe1-N1 98.34(5), N3-Fe1-N2 72.63(5), N5-Fe1-N2 91.37(5), N3-Fe1-N1 78.06(5), N3-Fe1-O1 92.08(5).

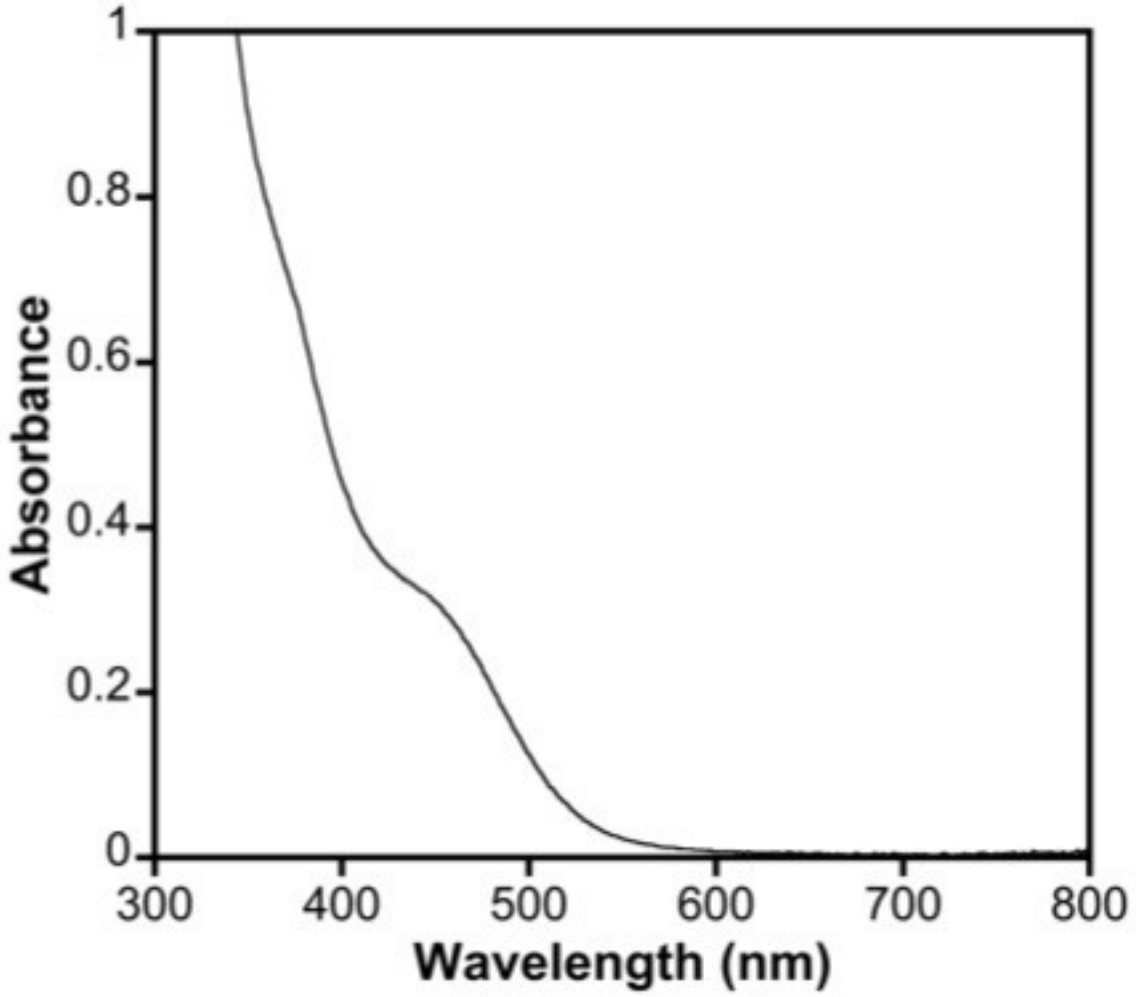

Figure S2. UV-vis spectrum of **1** (0.3 mM) in acetonitrile.

Crystal Structure of 2. The asymmetric unit contains one Fe complex, one ClO_4^- counterion and some amount of lattice solvent molecules (water and diethyl ether). The perchlorate counterion is disordered over three orientations, and the occupancy factors of the three components refine to 0.465(3), 0.231(2) and 0.304(3). One molecule of diethyl ether is found at sites of inversion symmetry, and thus is disordered with an occupancy factor refining to 0.381(4). The lattice water solvent molecule is disordered over two orientations, and the occupancy factor of the major component refines to 0.769(7).

2, Fw = 764.13, black rod, 0.32 × 0.09 × 0.05 mm^3, triclinic, *P*-1 (no. 2), a = 10.0679(4), b = 12.6568(4), c = 15.6766(5) Å, α = 98.834(3), β = 106.858(3), γ = 104.372(3)°, V = 1796.30(11) $Å^3$, Z = 2, D_x = 1.413 g cm^{-3}, μ = 4.527 mm^{-1}, T_{min}-T_{max}: 0.383–0.816. 23559 Reflections were measured up to a resolution of $(\sin\theta/\lambda)_{max}$ = 0.62 $Å^{-1}$. 7075 Reflections were unique (R_{int} = 0.0255), of which 6418 were observed [$I > 2\sigma(I)$]. 591 Parameters were refined using 426 restraints. $R1/wR2$ [$I > 2\sigma(I)$]: 0.0504/0.1410. $R1/wR2$ [all refl.]:
0.0555/0.1461. S = 1.026. Residual electron density found between −0.49 and 0.90 e $Å^{-3}$.

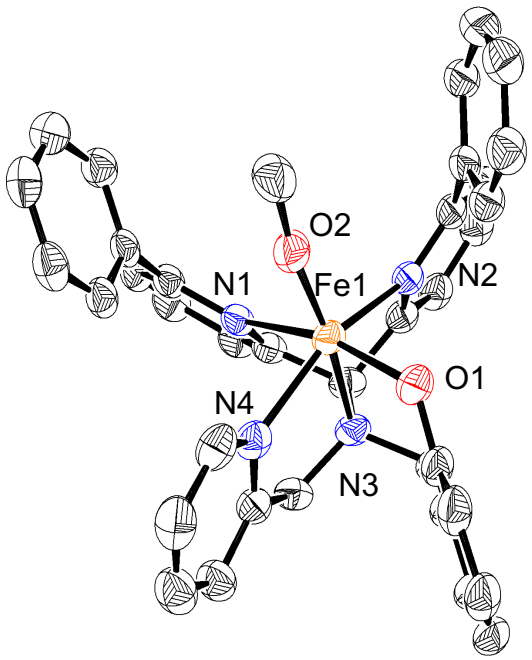

Figure S3. Displacement ellipsoid plot (50% probability level) of the cation of **2**. H atoms, lattice solvent molecules, and ClO_4^- counterion have been omitted for clarity. Selected bond distances (Å) and angles (°): Fe1-N1 2.341(2), Fe1-N2 2.249(2), Fe1-N3 2.202(2),

Fe1-N4 2.156(2), Fe1-O1 1.9279(18), Fe1-O2 1.785(2), N1-Fe1-N2 81.41(7), N1-Fe1-N3 73.69(8), N1-Fe1-N4 87.28(7), N1-Fe1-O1 162.73(8), N1-Fe1-O2 94.40(9), N2-Fe1-N3 75.91(8), N2-Fe1-N4 152.29(8), N2-Fe1-O1 98.27(8), N2-Fe1-O2 102.40(9), N3-Fe1-N4 76.67(8), N3-Fe1-O1 89.43(8), N3-Fe1-O2 168.08(9), N4-Fe1-O1 85.26(9), N4-Fe1-O2 103.63(9), O1-Fe1-O2 102.48(9).

VI. Supporting Tables

Table S1. ^{57}Fe Mössbauer parameters for **1**, **2** and reaction of **2** with $Ph_3C\bullet$ in THF.

	T (K)	Species	δ (mm/s)	ΔE_Q (mm/s)	$\Gamma_{L(R)}$ (mm/s)	B_{int} (T)	I (%)
1	5.2[a]	hs-Fe^{II}	1.05	2.29	0.31 (0.34)	-	90
2	5.2[b]	hs-Fe^{III} fast relaxing	0.50	1.29	0.66 (0.66)	-	30
		hs-Fe^{III} slow relaxing	0.50	-	0.50 (0.50)	49	70
	100[c]	hs-Fe^{III}	0.48	1.05	0.82 (0.93)	-	90
	100[d]	hs-Fe^{III}	0.45	0.84	0.54 (0.56)	-	
Reaction of **2** with $Ph_3C\bullet$	5.1[a]	hs-Fe^{II}	1.37	3.34	0.40 (0.45)	-	90

[a] Spectrum contains approximately 10 % iron(III).

[b] Spectra are a mixture of the fast- and slow-relaxing regimes.

[c] Spectrum is *nearly* completely fast-relaxing HS iron(III). Both isomer shift and quadrupole splitting have decreased due to a second order Doppler effect. Line broadening shows the sample is not fully relaxed.

[d] Spectrum measured using crystalline **2** suspended in boron-nitride.

Table S2: Comparison of the metrical parameters obtained from X-ray crystallography and DFT calculations for **1-MeCN**, **1-THF**, **1-5C** (the five-coordinate analog of complex **1** without the CH_3CN ligand), and **2**.

	1-MeCN		1-THF	1-5C	2	
Bond Distances (Å)	**XRD**	**DFT**	**DFT**	**DFT**	**XRD**	**DFT**
Fe1-O1	1.9560(13)	1.945	1.955	1.907	1.9279(18)	1.933
Fe1-N1	2.2633(13)	2.253	2.281	2.152	2.341(2)	2.390
Fe1-N2	2.473(3)	2.522	2.479	2.267	2.249(2)	2.259
Fe1-N3	2.1699(13)	2.186	2.162	2.133	2.202(2)	2.214
Fe1-N4	2.1598(14)	2.178	2.211	2.160	2.156(2)	2.157
Fe1-L (N5/O2)	2.0769(14)	2.012	2.114	-----	1.785(2)	1.787
Bond Angles (°)						
O1-Fe1-N1	99.71(5)	97.65	97.22	99.94	162.73(8)	161.88
O1-Fe1-N2	164.43(5)	165.04	168.06	173.98	98.27(8)	96.68
O1-Fe1-N3	92.08(5)	91.87	93.21	94.28	89.43(8)	88.29
O1-Fe1-N4	88.82(6)	89.25	87.42	89.42	85.26(9)	84.62
O1-Fe1-L	103.96(6)	102.08	95.04	-----	102.48(9)	101.52
N1-Fe1-N4	155.78(5)	156.36	156.25	160.73	87.28(7)	89.46
N2-Fe1-N4	85.40(5)	88.23	89.07	89.98	152.29(8)	153.48
N3-Fe1-N4	79.02(5)	78.69	78.34	80.37	76.67(8)	77.35
N1-Fe1-L	98.34(5)	101.56	99.66	-----	94.40(9)	96.53
N2-Fe1-L	91.37(5)	92.67	96.87	-----	102.40(9)	101.53
N3-Fe1-L	163.95(5)	165.86	171.67	-----	168.08(9)	170.16
N4-Fe1-L	101.54(5)	99.02	103.13	-----	103.63(9)	104.15
N1-Fe1-N2	80.41(5)	79.27	81.61	78.94	81.41(7)	81.14
N1-Fe1-N3	78.06(5)	78.51	78.15	82.16	73.69(8)	73.69
N2-Fe1-N3	72.63(5)	73.17	74.90	79.71	75.91(8)	76.21

Table S3: Calculated Mössbauer parameters **1-MeCN**, **1-THF**, **1-5C**, and **2**.

Complex[a]	Isomer Shift[b] (mm/s^{-1})	Quadrupole Splitting (mm/s^{-1})
1-MeCN	1.05	3.62
1-THF	1.15	3.50
1-5C	1.02	2.74
2	0.61	1.60

[a] See DFT computational section for details regarding geometry optimizations

[b] ρ (0) calculated using the B3LYP functional with a combination of CP(PPP) for Fe and def2-TZVP for all other atoms and calibrated as described in DFT computational section.

Table S4: Optimized coordinates for **1-MeCN**.

Fe	0.522849	2.592136	12.897903
C	-2.404920	-1.088544	14.112118
H	-3.313941	-0.739325	14.613279
C	-2.448936	-2.241543	13.315974
H	-3.390418	-2.790097	13.207107
C	-1.288104	-2.690604	12.662111
H	-1.317597	-3.599637	12.052296
C	-0.089383	-1.970257	12.800546
H	0.820109	-2.319630	12.300203
C	-0.043672	-0.805779	13.583319
H	0.894968	-0.250112	13.683761
C	-1.203581	-0.354848	14.250063
C	-1.172223	0.822142	15.161413
C	-1.758099	0.695779	16.441777
H	-2.212890	-0.255773	16.727615
C	-1.716652	1.762933	17.342384
H	-2.149608	1.667442	18.342244
C	-1.091159	2.951495	16.942126
H	-1.021685	3.812981	17.612785
C	-0.545498	3.018340	15.655042
C	0.028705	4.336591	15.128276
H	0.233046	5.008458	15.984872
C	-1.068453	4.949904	14.261072
C	-1.924962	5.921431	14.797744
H	-1.738443	6.331466	15.793551
C	-3.019969	6.337220	14.030019
H	-3.714817	7.092543	14.410005
C	-3.197366	5.780720	12.760785
H	-4.025756	6.100667	12.122859
C	-2.269175	4.834513	12.269541
C	-2.435901	4.323111	10.882292
C	-1.353934	4.322601	9.978361
H	-0.377625	4.671756	10.320478
C	-1.530843	3.891753	8.656058
H	-0.682261	3.884320	7.964865
C	-2.793679	3.454470	8.220163
H	-2.924366	3.108944	7.189794
C	-3.880937	3.458674	9.111435
H	-4.866812	3.116681	8.779468
C	-3.705851	3.896624	10.432970
H	-4.552547	3.885252	11.127993
C	1.780347	5.270410	13.626124
H	2.561755	5.771039	14.226237
H	0.956382	5.994980	13.506042

C	2.311770	4.920978	12.247629
C	3.338452	5.664741	11.644292
H	3.813798	6.483253	12.193172
C	3.742827	5.338129	10.343698
H	4.542353	5.903243	9.854768
C	3.111646	4.271412	9.683823
H	3.392203	3.979133	8.669003
C	2.097812	3.578966	10.353868
H	1.569383	2.748704	9.875275
C	2.319552	3.453628	15.199078
H	1.833266	2.624491	15.741161
H	2.644566	4.201168	15.951010
C	3.511629	2.927374	14.438092
C	4.814049	3.357777	14.747900
H	4.945178	4.146368	15.500131
C	5.937579	2.788249	14.127737
H	6.944293	3.133903	14.383458
C	5.750473	1.765324	13.178931
H	6.618037	1.306820	12.690543
C	4.462511	1.325122	12.848383
H	4.308718	0.529823	12.110454
C	3.317110	1.895277	13.464777
N	-0.578879	1.987371	14.767269
N	-1.218353	4.412616	13.026679
N	1.256465	4.069213	14.333025
N	1.694746	3.897359	11.606076
N	-0.493126	1.580438	11.486105
C	-0.980626	0.920625	10.652883
C	-1.587052	0.085057	9.631023
H	-1.528400	-0.973870	9.937337
H	-1.066382	0.213444	8.664338
H	-2.648061	0.359674	9.509123
O	2.093930	1.473002	13.149683
O	1.652538	1.107743	4.914532
O	0.221695	0.266205	6.743781
O	-0.372351	2.360462	5.570358
Cl	0.771195	1.512693	6.077439
O	1.588445	2.299419	7.076824

Table S5: Optimized coordinates for **1-THF**.

Fe	0.356471	2.649535	12.848095
C	-2.291599	-1.298712	14.430216
H	-3.219188	-0.987655	14.922256
C	-2.236414	-2.537767	13.777829
H	-3.118058	-3.187476	13.773135
C	-1.053067	-2.943783	13.136494
H	-1.003369	-3.917596	12.638845
C	0.064218	-2.091871	13.139217
H	0.991230	-2.404236	12.646812
C	0.009814	-0.841820	13.775320
H	0.887486	-0.186610	13.764513
C	-1.169190	-0.434089	14.436630
C	-1.215640	0.817721	15.241331
C	-1.789657	0.738236	16.530368
H	-2.197191	-0.217349	16.868508
C	-1.786719	1.845914	17.381385
H	-2.213967	1.783373	18.386106
C	-1.181685	3.023385	16.926067
H	-1.112119	3.911607	17.561013
C	-0.644482	3.046725	15.634287
C	-0.041199	4.341055	15.097032
H	0.194553	5.005063	15.952651
C	-1.106772	5.010999	14.235686
C	-1.859026	6.066403	14.768756
H	-1.624968	6.458439	15.761740
C	-2.898904	6.599682	13.998906
H	-3.504645	7.431117	14.371883
C	-3.125815	6.063983	12.729997
H	-3.900725	6.482179	12.082840
C	-2.316801	5.010529	12.244213
C	-2.558433	4.524587	10.860119
C	-1.485999	4.239945	9.989543
H	-0.464245	4.345807	10.357939
C	-1.723806	3.862865	8.660097
H	-0.880807	3.644877	7.996816
C	-3.041916	3.754520	8.184499
H	-3.224126	3.453021	7.148085
C	-4.119824	4.026202	9.044691
H	-5.149890	3.932820	8.684523
C	-3.882198	4.415311	10.370146
H	-4.728523	4.611066	11.037015
C	1.741110	5.242742	13.626054

H	2.533041	5.696629	14.249828
H	0.941624	5.996856	13.522884
C	2.273118	4.910163	12.247467
C	3.361552	5.602306	11.696956
H	3.874406	6.365770	12.289890
C	3.783836	5.292504	10.397543
H	4.633164	5.817419	9.949868
C	3.103217	4.290281	9.691782
H	3.387143	4.002569	8.676761
C	2.025589	3.648815	10.311754
H	1.473302	2.870930	9.779246
C	2.220325	3.340226	15.112020
H	1.709705	2.511464	15.629987
H	2.590579	4.042160	15.887739
C	3.376586	2.803175	14.303227
C	4.698251	3.175759	14.609351
H	4.868259	3.918671	15.399526
C	5.792075	2.605857	13.940324
H	6.813425	2.906807	14.194507
C	5.555973	1.641023	12.942765
H	6.399562	1.184447	12.412615
C	4.250108	1.256242	12.617262
H	4.056595	0.507906	11.841112
C	3.132002	1.825278	13.283616
N	-0.676909	1.989300	14.771350
N	-1.314982	4.473651	13.005288
N	1.172571	4.038695	14.290232
N	1.600194	3.948690	11.562675
O	1.894304	1.448457	12.970488
O	-0.696933	1.460809	11.453162
C	-2.130217	1.148284	11.503956
H	-2.310578	0.538466	12.404243
C	-2.418491	0.369778	10.219884
H	-3.281292	-0.306163	10.335505
C	-1.092533	-0.378771	9.980175
H	-1.030042	-1.271815	10.623416
H	-0.952493	-0.679229	8.930307
H	-2.624107	1.066102	9.390284
H	-2.672422	2.101129	11.578158
C	-0.052282	0.660304	10.397236
H	0.871110	0.246473	10.829855
H	0.192113	1.331320	9.556444
O	1.810482	1.615767	5.158820
O	0.587295	0.242009	6.813454
O	-0.545923	2.136048	5.699244
Cl	0.767792	1.636273	6.254020

O 1.233039 2.566556 7.361764

Table S6: Optimized coordinates for **1-5C**.

Fe	0.579904	2.883834	12.890452
C	-2.459299	-0.809284	13.449367
H	-3.224471	-0.714329	14.227514
C	-2.714531	-1.595699	12.317830
H	-3.667116	-2.129216	12.233857
C	-1.761500	-1.682171	11.288472
H	-1.966433	-2.287627	10.399307
C	-0.544365	-0.991903	11.404347
H	0.206220	-1.056109	10.609951
C	-0.282432	-0.205532	12.537145
H	0.705218	0.253577	12.649847
C	-1.243366	-0.095640	13.568532
C	-1.036457	0.781575	14.747297
C	-1.494230	0.397784	16.029483
H	-1.917103	-0.599969	16.169306
C	-1.393749	1.284716	17.103383
H	-1.736995	0.991191	18.099647
C	-0.851311	2.562671	16.884135
H	-0.779767	3.297332	17.691270
C	-0.393644	2.874268	15.602279
C	0.108068	4.272617	15.229797
H	0.259162	4.876514	16.144770
C	-0.973072	4.913987	14.355110
C	-1.756611	5.977558	14.812220
H	-1.577255	6.415598	15.797396
C	-2.755431	6.469728	13.958585
H	-3.365635	7.328564	14.253607
C	-2.965147	5.847880	12.727045
H	-3.736389	6.228574	12.054595
C	-2.171651	4.740181	12.341356
C	-2.457039	3.990375	11.089967
C	-1.511956	3.115979	10.509292
H	-0.513531	3.023609	10.958426
C	-1.794541	2.399112	9.341045
H	-1.035555	1.737621	8.913365
C	-3.047294	2.542815	8.722876
H	-3.272240	1.990461	7.805211
C	-4.008458	3.396265	9.289240
H	-4.993155	3.503471	8.822956
C	-3.720101	4.109204	10.459374
H	-4.500835	4.738251	10.896193
C	1.830041	5.441840	13.845900
H	2.662754	5.852816	14.444329
H	1.004364	6.173062	13.905512

C	2.247352	5.293081	12.392013
C	3.209959	6.140092	11.822766
H	3.698764	6.900374	12.439551
C	3.542525	5.984474	10.470877
H	4.295144	6.630141	10.007534
C	2.911324	4.973112	9.732058
H	3.155278	4.791684	8.682266
C	1.958020	4.171029	10.367997
H	1.467811	3.358163	9.822042
C	2.460174	3.430806	15.148498
H	1.997459	2.538428	15.603956
H	2.828951	4.074604	15.972127
C	3.606634	3.020371	14.252697
C	4.925779	3.405594	14.553184
H	5.102872	4.060074	15.415833
C	6.010265	2.955124	13.784593
H	7.030050	3.262942	14.036484
C	5.769480	2.104513	12.689392
H	6.606313	1.747448	12.078888
C	4.465619	1.709495	12.365843
H	4.262177	1.056737	11.510502
C	3.363198	2.153116	13.139211
N	-0.455960	2.001668	14.558132
N	-1.148845	4.328514	13.142178
N	1.360517	4.149329	14.420446
N	1.612843	4.334118	11.667743
O	2.122684	1.763749	12.831216
O	2.271341	0.040743	6.623198
O	2.361386	-0.141090	9.089365
O	0.182837	-0.201380	7.923673
Cl	1.573177	0.397671	7.918540
O	1.465246	1.907392	8.025718

Table S7: Optimized coordinates for **2**.

Fe	-2.723509	0.514255	10.032258
C	-6.237398	3.326358	11.936633
H	-7.141479	2.727158	12.009646
C	-6.325517	4.679803	11.604157
H	-7.298806	5.127607	11.424210
C	-5.164939	5.454754	11.504000
H	-5.233188	6.509394	11.252386
C	-3.915739	4.867634	11.735601
H	-3.012423	5.468424	11.675727
C	-3.825701	3.511507	12.056203
H	-2.862023	3.063108	12.266344
C	-4.984242	2.726618	12.154308
C	-4.918098	1.309894	12.596491
C	-5.742411	0.915295	13.665710
H	-6.406968	1.645057	14.115034
C	-5.665674	-0.378375	14.168868
H	-6.278860	-0.682646	15.011244
C	-4.769797	-1.270014	13.579378
H	-4.663176	-2.288080	13.937893
C	-4.008479	-0.822505	12.502894
C	-3.133470	-1.791297	11.723379
H	-2.918860	-2.676020	12.334821
C	-3.945330	-2.196850	10.499107
C	-4.652138	-3.394215	10.474814
H	-4.557023	-4.101692	11.292067
C	-5.477507	-3.650798	9.378681
H	-6.043552	-4.574678	9.316041
C	-5.545346	-2.709132	8.358714
H	-6.151651	-2.892559	7.478820
C	-4.788180	-1.524884	8.432521
C	-4.845159	-0.576906	7.291078
C	-6.091802	-0.285825	6.705489
H	-7.001500	-0.687136	7.144517
C	-6.170651	0.535568	5.579881
H	-7.140108	0.762697	5.145827
C	-5.004080	1.061393	5.014262
H	-5.062896	1.690819	4.130542
C	-3.762051	0.770700	5.588936
H	-2.853001	1.171452	5.149067
C	-3.677752	-0.038060	6.724682
H	-2.709953	-0.258865	7.163002
C	-1.109469	-0.546089	12.418157
H	-0.339901	-1.253917	12.744839
H	-1.786340	-0.387714	13.263815
C	-0.490263	0.780976	12.040563
C	0.692099	1.246653	12.622470
H	1.223331	0.628135	13.338813
C	1.173525	2.503311	12.260101

H	2.091215	2.884064	12.696637
C	0.467923	3.258538	11.317076
H	0.815855	4.234201	10.998014
C	-0.698225	2.726526	10.779840
H	-1.285802	3.256667	10.037912
C	-1.040069	-2.053248	10.474100
H	-1.689693	-2.463901	9.695103
H	-0.717872	-2.878988	11.122380
C	0.144445	-1.375605	9.843004
C	1.448499	-1.840066	10.048964
H	1.611290	-2.674745	10.728333
C	2.532650	-1.255013	9.387728
H	3.540032	-1.625188	9.556068
C	2.304421	-0.187728	8.508637
H	3.135914	0.282455	7.990648
C	1.012496	0.290403	8.290785
H	0.833818	1.122118	7.615395
C	-0.088448	-0.294029	8.952330
C	-4.721183	2.566346	8.781779
H	-4.703028	2.626241	7.684504
H	-4.696581	3.582779	9.196907
H	-5.662924	2.090233	9.088707
N	-4.064153	0.433528	12.008936
N	-4.003355	-1.273580	9.511804
N	-1.890783	-1.112563	11.282198
N	-1.175711	1.520926	11.147810
O	-1.320186	0.167513	8.748423
O	-3.618468	1.838895	9.233624
O	4.726014	4.428198	6.094725
O	3.010595	2.757012	6.574389
Cl	3.859221	3.361388	5.502358
O	4.721586	2.306077	4.887253
O	2.980544	3.961455	4.449706

VII. Supporting Figures.

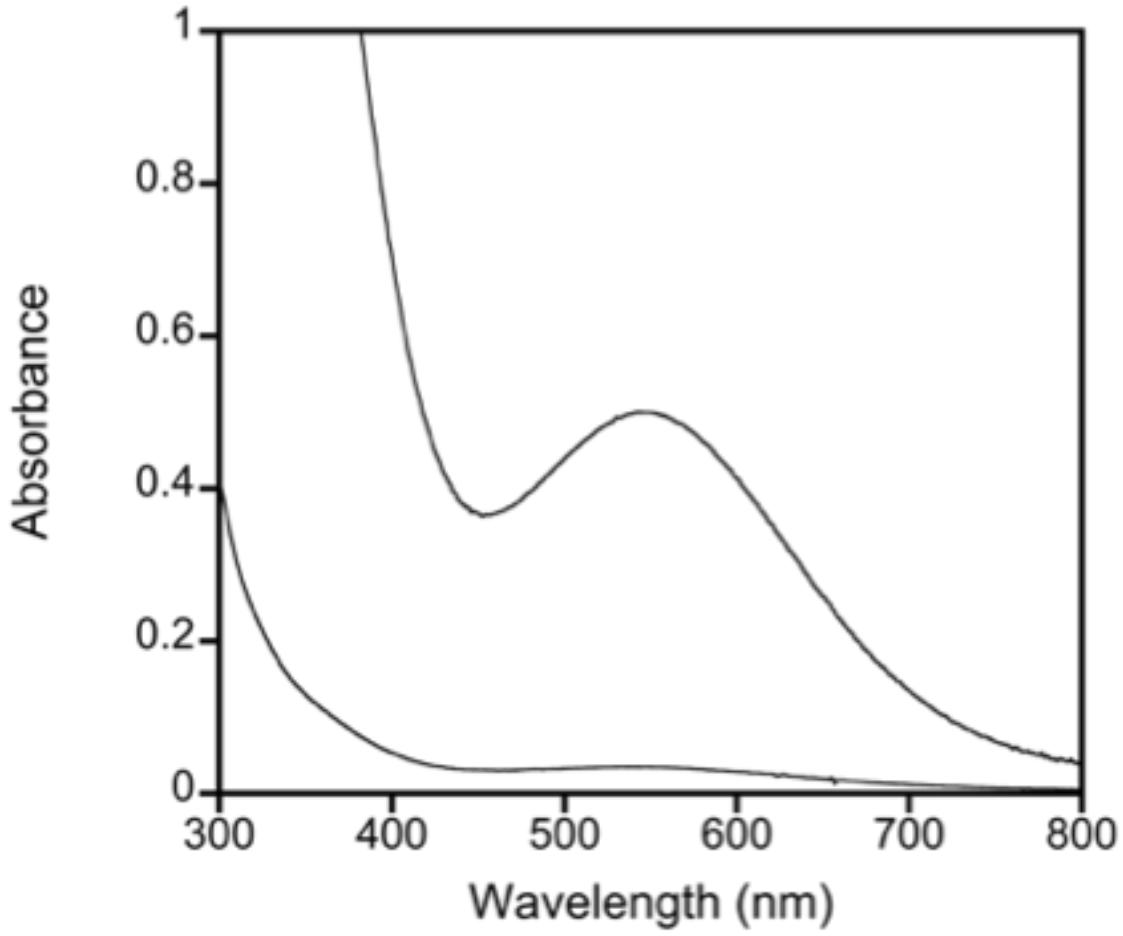

Figure S4. UV-vis spectra of **2** in methanol. Concentrated spectrum: 0.4 mM. Dilute spectrum: 0.03 mM.

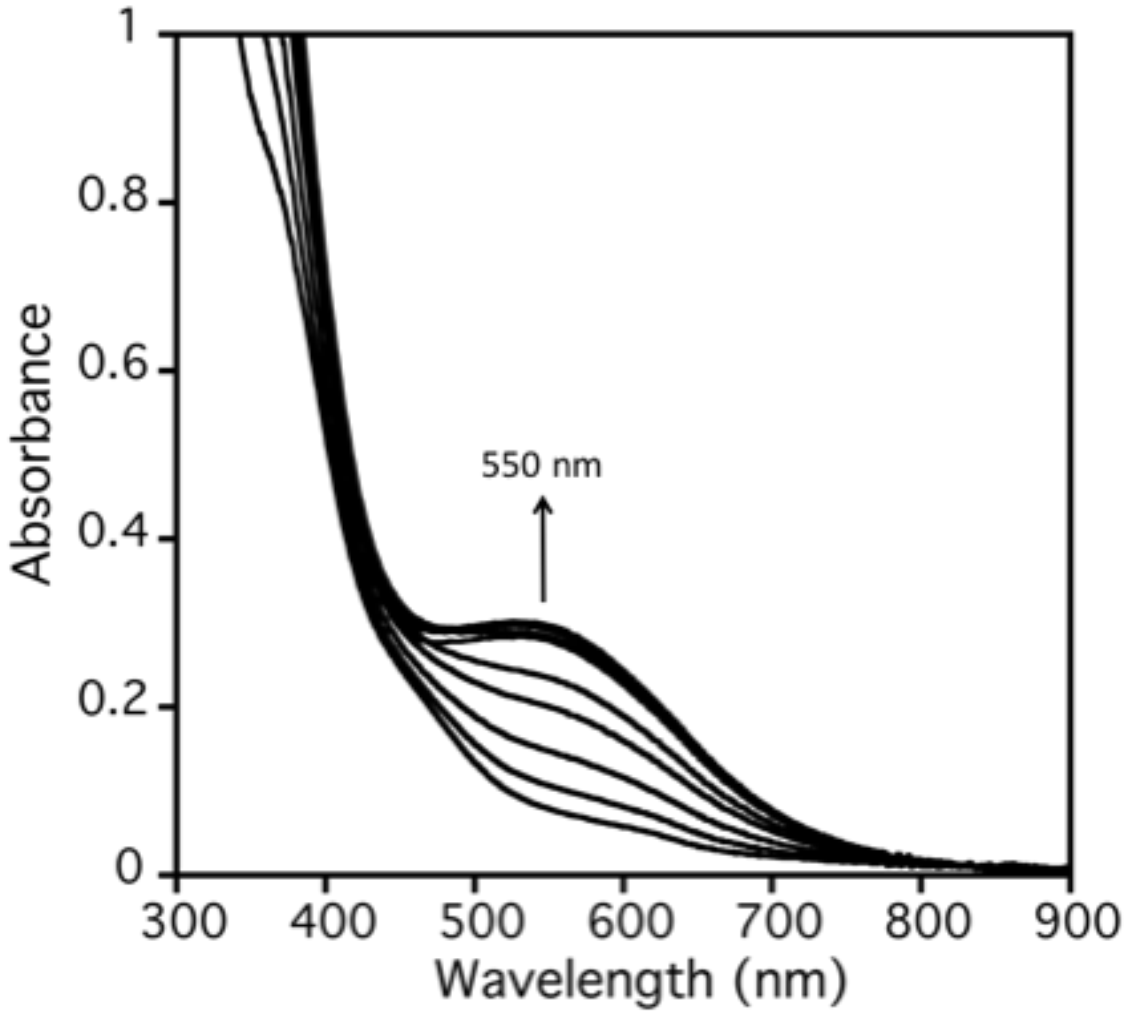

Figure S5. Formation of **2** from **1** (0.25 mM) in methanol at 23 °C under aerobic conditions, monitored by UV-vis spectroscopy over 8 h.

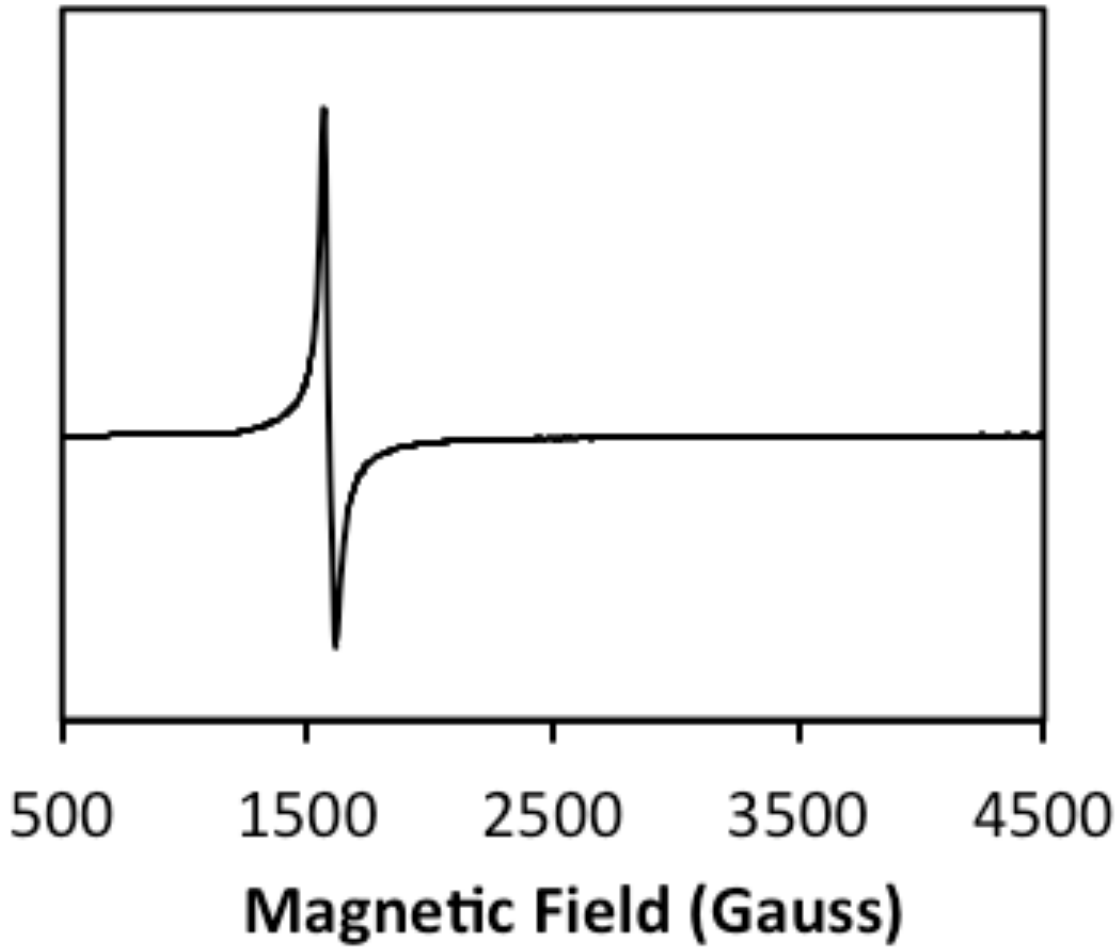

Figure S6. EPR spectrum of **2** in THF at 13 K. Frequency 9.2617 GHz, modulation amplitude 10 G, modulation frequency 100 KHz, attenuation 20 dB, receiver gain 5.02 x 10^3.

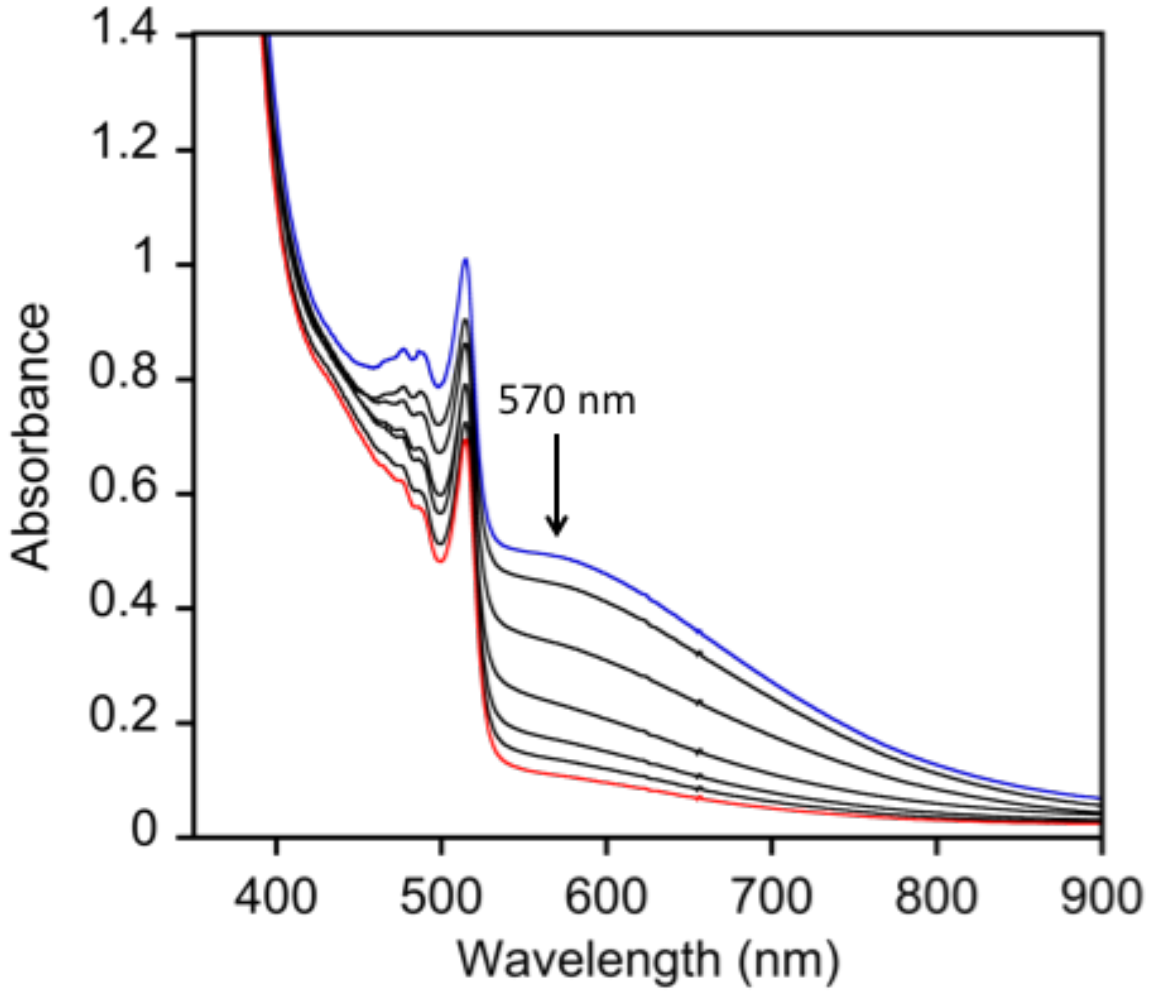

Figure S7. Reaction of **2** and $(Ph_3C)_2$ in THF at 50 °C, monitored by UV-vis spectroscopy. **2** (570 nm) is consumed over the course of 1 h. Initial spectrum (blue): combination of **2** and $(Ph_3C)_2$. Final spectrum (red): **2** has been consumed while excess $(Ph_3C)_2$ is still present.

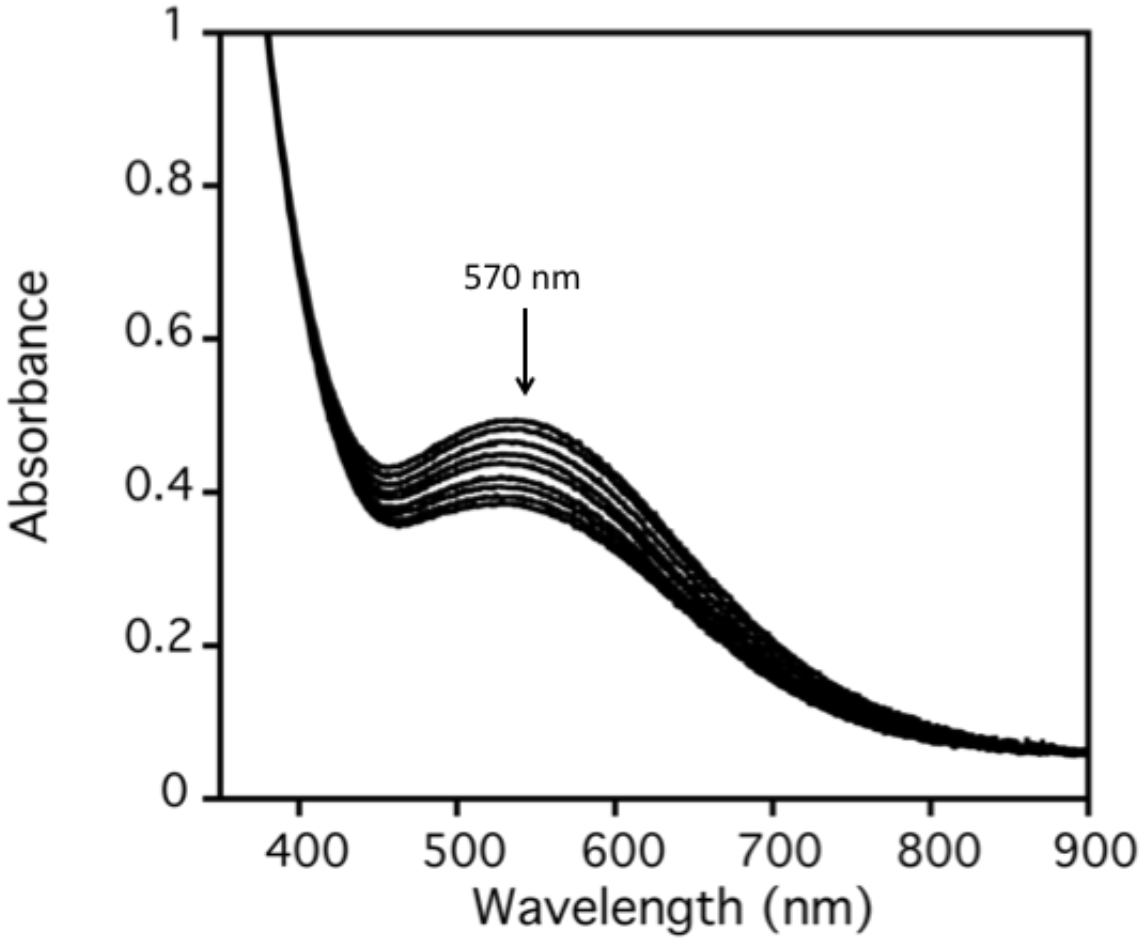

Figure S8. UV-vis spectra for complex **2** (0.4 mM) dissolved in THF at 50 °C over 1 h.

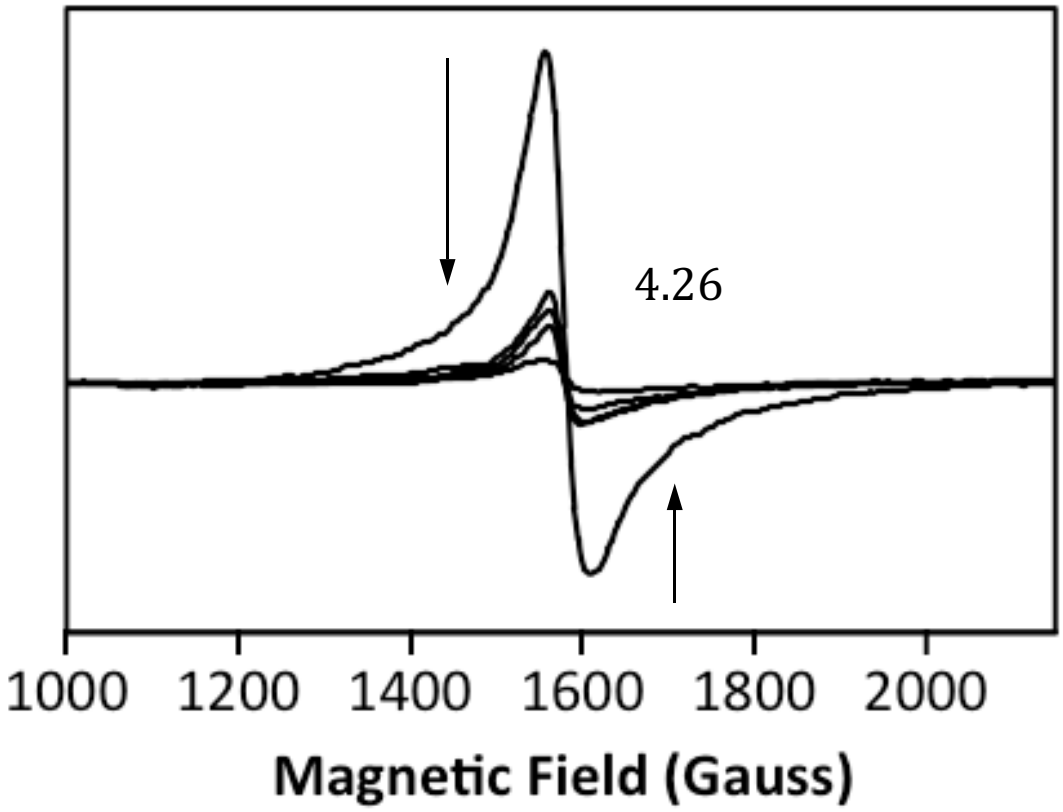

Figure S9. X-band EPR spectra at 13 K of the reaction of **2** and $(Ph_3C)_2$ (1.6 equiv) over 60 min in THF at 50 °C. Spectra were taken at 0, 1, 5, 30, and 60 min, showing up to 80% consumption of **2**. Frequency 9.2464 GHz, modulation amplitude 10 G, modulation frequency 100 KHz, attenuation 20 dB, power = 2.0 mW, receiver gain 5.02 x 10^3.

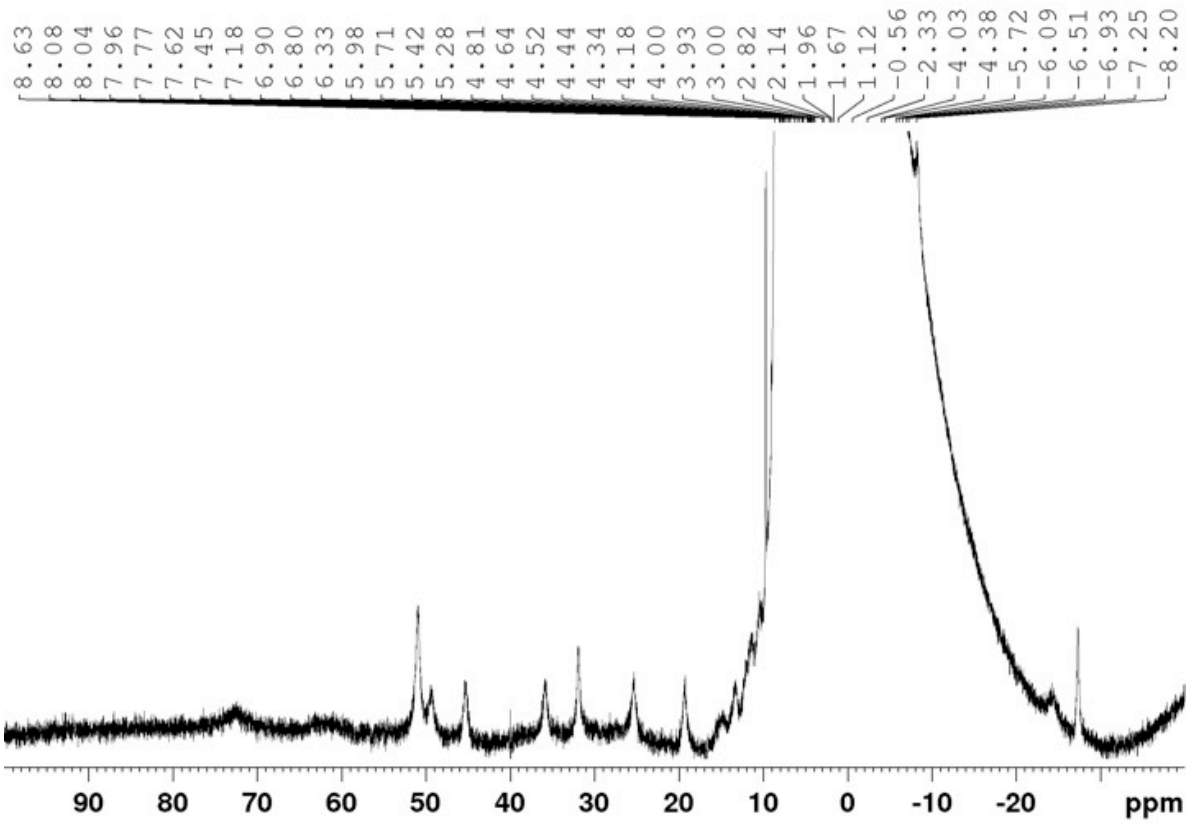

Figure S10. ^{1}H NMR spectrum of [Fe^{II}(N3PyO^{2Ph})(CH_3CN)](ClO_4) (**1**) in CD_3CN.

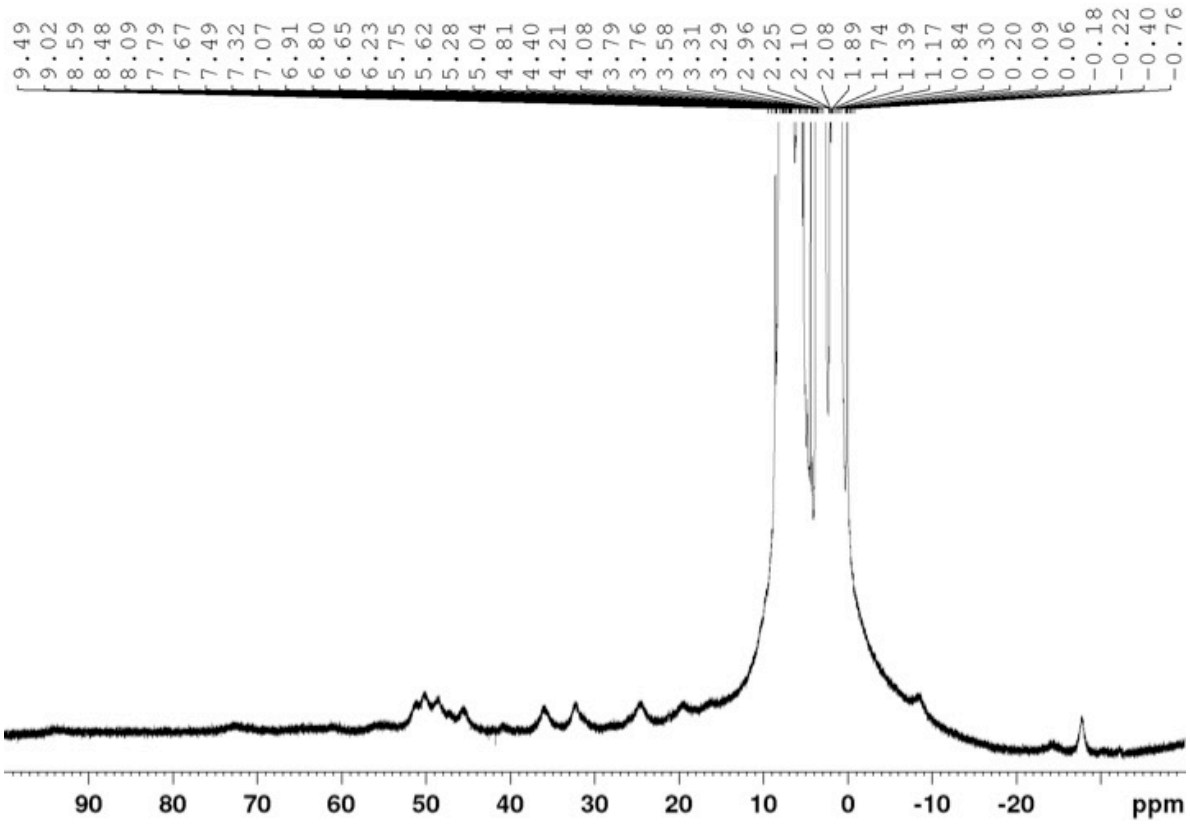

Figure S11. ^{1}H NMR spectrum of [Fe^{II}(N3PyO^{2Ph})(CH_3CN)](ClO_4) (**1**) in THF-d_8/CD_3CN.

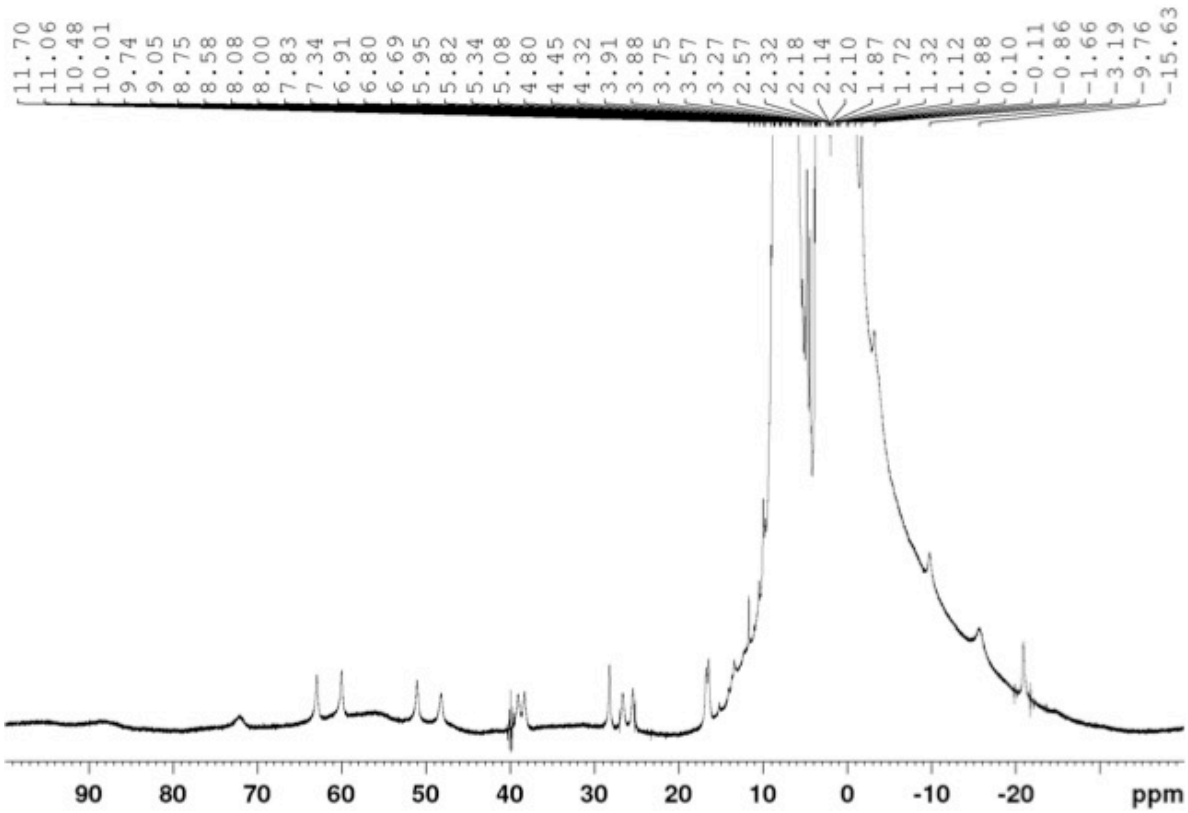

Figure S12. ^{1}H NMR spectrum of ([Fe^{III}(N3PyO^{2Ph})(OCH_3)](ClO_4) (**2**) in THF-d_8.

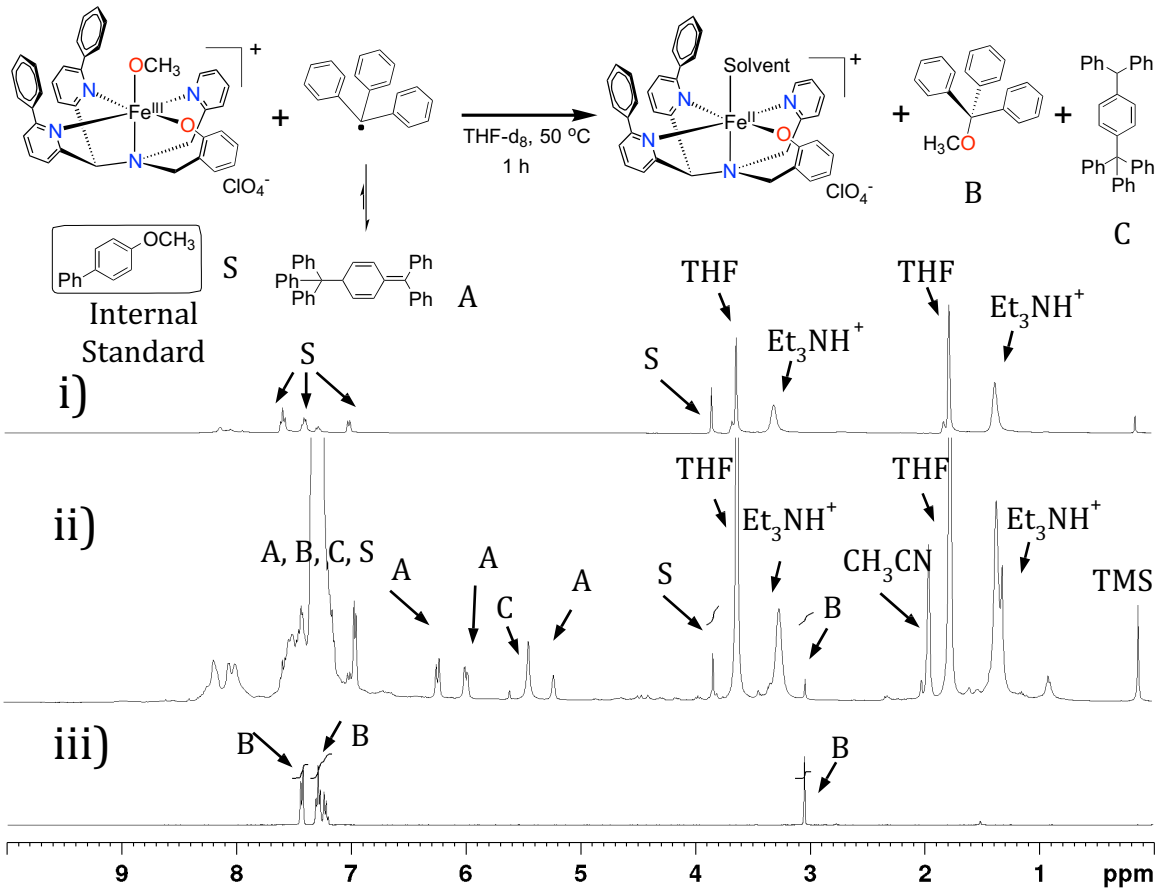

Figure S13. Reaction of **2** + $(Ph_3C)_2$ in THF-d_8 for 60 min at 50 °C as monitored by ^{1}H NMR spectroscopy. i) **2** + 4-Ph-C_6H_4-OCH_3 (internal standard S) before addition of $(Ph_3C)_2$. ii) **2** + $(Ph_3C)_2$ after 60 min. iii) Ph_3COCH_3 reference spectrum. Following the reaction, the –OCH_3 peak of the product Ph_3COCH_3 at 3.04 ppm was integrated against the internal standard (4-Ph-C_6H_4-OCH_3) –OCH_3 peak at 3.83 ppm. Peaks at 5.2, 6.0, and 6.2 ppm were from unreacted $(Ph_3C)_2$. The peak at 5.4 ppm is assigned to Ph_3-C_6H_4-$CHPh_2$, a side-product of trityl radical recombination.[23] Acetonitrile and Et_3NH^+ may be observed as residual compounds from in-situ generation of **2** (see experimental section for details).

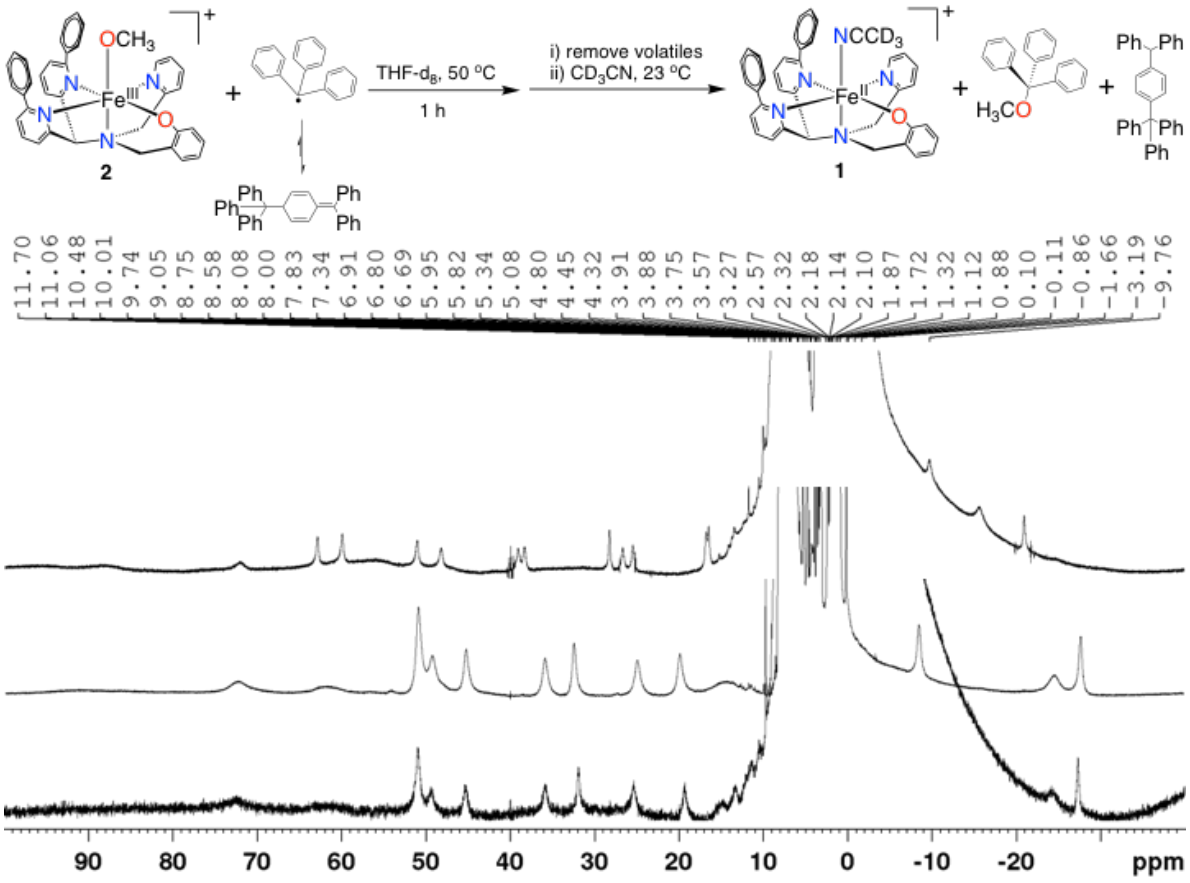

Figure S14. ^{1}H NMR spectra of [Fe^{III}(N3PyO^{2Ph})(OMe)](ClO_4) (**2**) + $(Ph_3C)_2$ in THF-d_8 for 60 min at 50 °C. Top: **2** before addition of $(Ph_3C)_2$. Middle: **2** + $(Ph_3C)_2$ after 60 min, followed by removal of THF-d_8 and dissolution in CD_3CN. Bottom: [Fe^{II}(N3PyO^{2Ph})(CH_3CN)](ClO_4) (**1**) in CD_3CN.

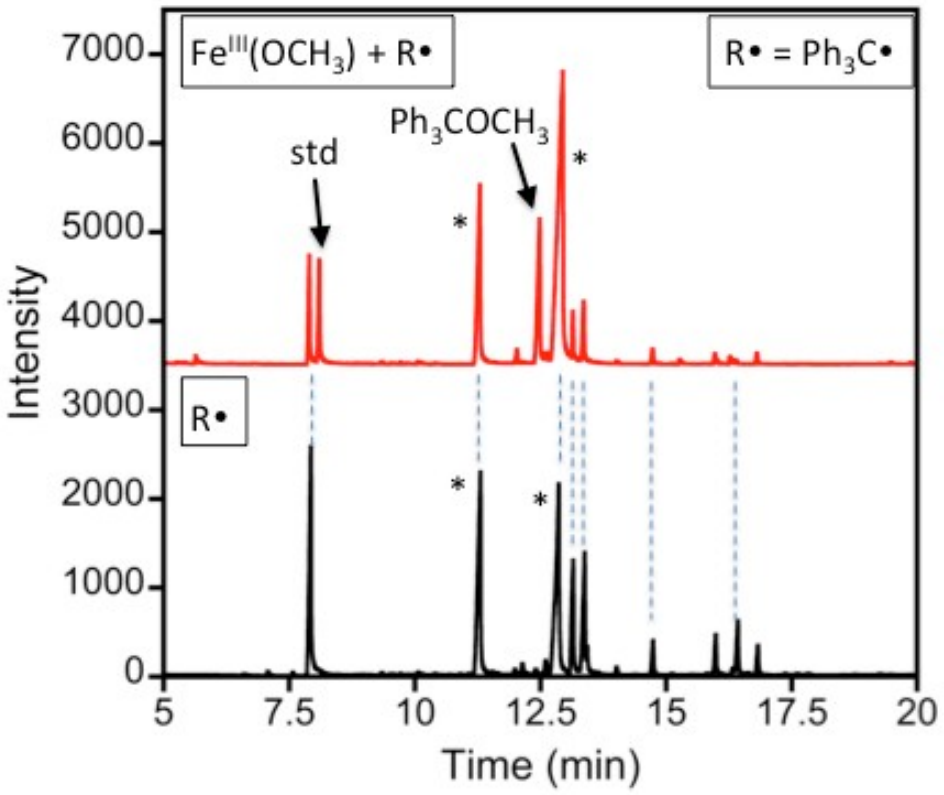

Figure S15. GC-FID data for the reaction of **2** (4 mM) and $(Ph_3C)_2$ (3 equiv) (red) and $(Ph_3C)_2$ alone (black). Data are offset to aid in viewing. The Ph_3COCH_3 (R_T = 12.4 min) was quantified from a calibration curve with the Ph-C_6H_4-OCH_3 internal standard (R_T = 8.1 min), yield = 58%. Marked peaks at 11.3 min and 12.9 min are from triphenyl methane (Ph_3CH) and triphenyl methanol (Ph_3COH) respectively, resulting from radical decay during aerobic workup. Unlabelled peaks are unidentified decay products, also present in $(Ph_3C)_2$ (shown by dashed lines).

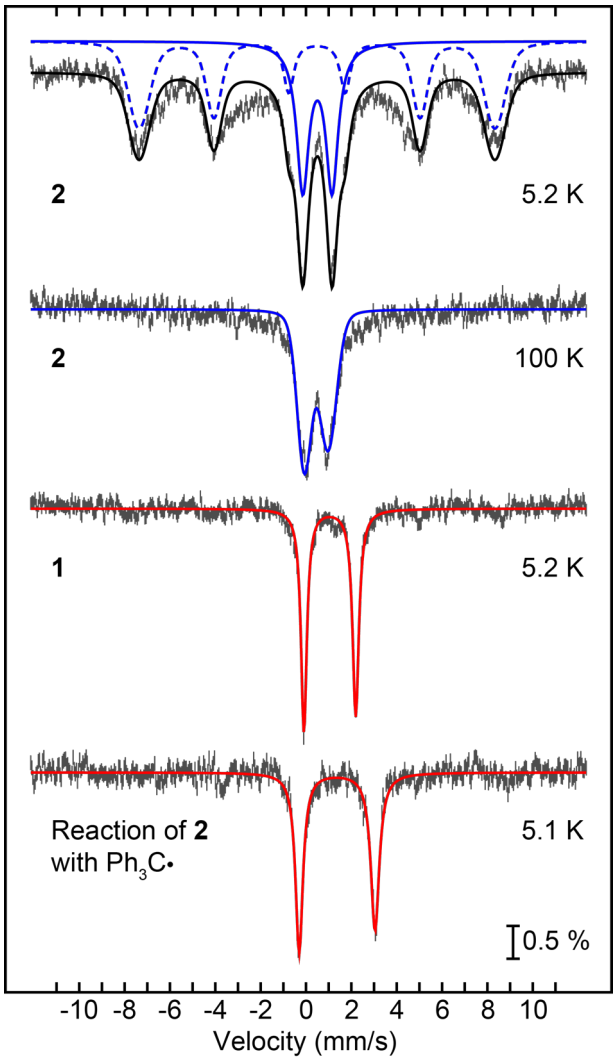

Figure S16. ^{57}Fe Mössbauer spectra for: **2 (**hatched line) together with the best fits for hs-Fe^{III} in both the slow-(blue dashed line) and fast-relaxing (blue solid line) regimes (top); same sample at 100 K showing the experimental data (hatched line) and best fit (blue line) for a fast-relaxing quadrupole doublet as the major component (top middle); **1** (hatched line) with best-fit line for Fe^{II} overlaid (red) (bottom middle); the reaction mixture of **2** and Gomberg's dimer in THF at 50 °C, frozen after 70 min, experimental (hatched line) and best fit for an Fe^{II} quadrupole doublet (red line) (bottom).

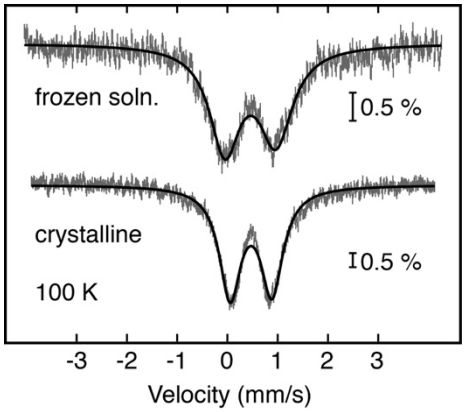

Figure S17. ^{57}Fe Mössbauer spectra of **2** in frozen solution (THF) (top) and as a crystalline solid dispersed in a boron nitride matrix (bottom). The two spectra are almost identical (see parameters in Table S1), providing strong evidence that complex **2** maintains its monomeric structure in solution.

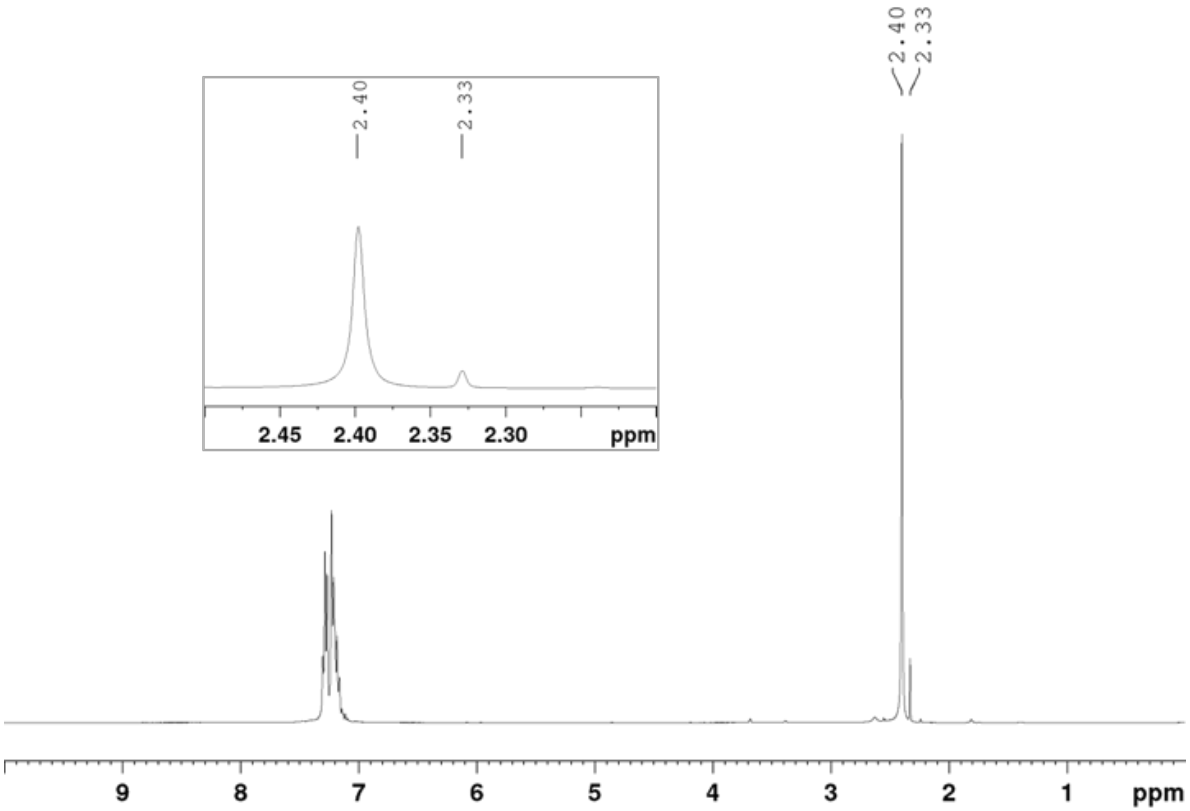

Figure S18. The ^{1}H NMR spectrum for the Evans method determination of the solution magnetic moment for **2** (0.0014 M) in THF-d_8 with toluene added as the internal standard. Inset: Expanded region of the spectrum showing the toluene –CH_3 peaks. $\Delta\nu$ = 28.01 Hz; f = 400.13 MHz; T = 294.8 K. The equation $\mu_{eff} = 0.0618(\Delta\nu T/2fM)^{1/2}$ was used to calculate the effective magnetic moment for **2**, where f is the oscillator frequency (MHz) of the superconducting spectrometer, T is temperature (K), M is the molar concentration of the paramagnetic metal complex, and $\Delta\nu$ is the frequency difference (Hz) between the two standard toluene -CH_3 signals.

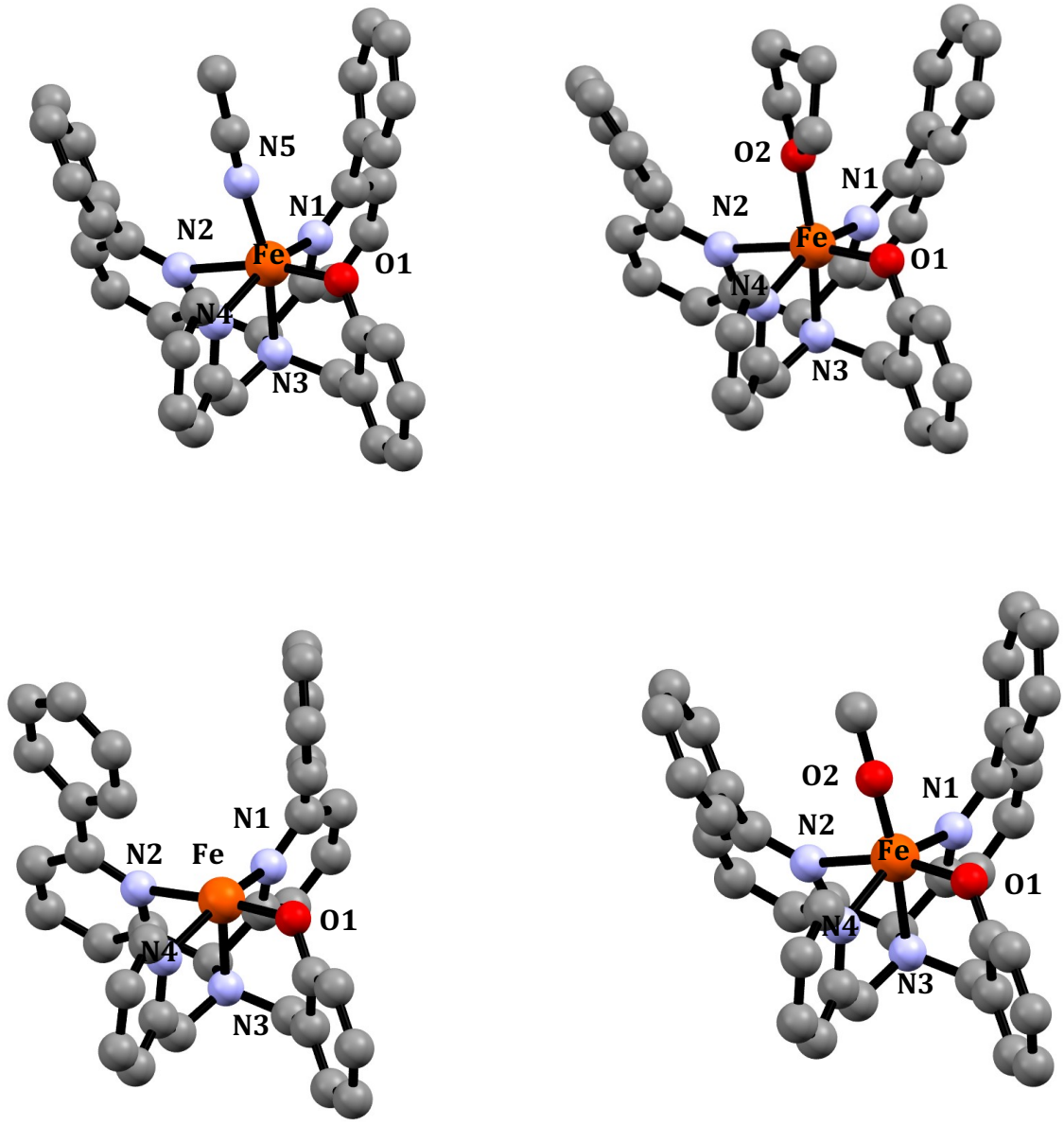

Figure S19: The gas phase optimized geometry for **1-MeCN** (top left), **1-THF** (top right), **1-5C** (bottom left), and **2** (bottom right) with hydrogen atoms and ClO_4^- counterion omitted.

VIII. References.

1. Sahu, S.; Widger, L. R.; Quesne, M. G.; de Visser, S. P.; Matsumura, H.; Moënne-Loccoz, P.; Siegler, M. A.; Goldberg, D. P., *J. Am. Chem. Soc.* **2013,** *135*, 10590-10593.
2. Ghosh, S.; Das, J., *Tetrahedron Lett.* **2011,** *52*, 1112-1116.
3. Jang, E. S.; McMullin, C. L.; Kass, M.; Meyer, K.; Cundari, T. R.; Warren, T. H., *J. Am. Chem. Soc.* **2014,** *136*, 10930-10940.
4. Gomberg, M., *J. Am. Chem. Soc.* **1900,** *22*, 757-771.
5. Gomberg, M., *J. Am. Chem. Soc.* **1914,** *36*, 1144-1170.
6. Ligtenbarg, A. G. J.; Oosting, P.; Roelfes, G.; La Crois, R. M.; Lutz, M.; Hage, R.; Spek, A. L.; Feringa, B. L., *Chem. Commun.* **2001**, 385-386.
7. Evans, D. F.; Jakubovik, D. A., *J. Chem. Soc. Dalton Trans.* **1988**, 2927-2933.
8. Confer, A. M.; McQuilken, A. C.; Matsumura, H.; Moënne-Loccoz, P.; Goldberg, D. P., *J. Am. Chem. Soc.* **2017,** *139*, 10621-10624.
9. Neese, F., *Wiley Interdiscip. Rev. Comput. Mol. Sci.* **2012,** *2*, 73-78.
10. Becke, A. D., *J. Chem. Phys.* **1986,** *84*, 4524-4529.
11. Perdew, J. P., *Phys. Rev. B* **1986,** *33*, 8822-8824.
12. Tao, J.; Perdew, J. P.; Staroverov, V. N.; Scuseria, G. E., *Phys. Rev. Lett.* **2003,** *91*, 1-4.
13. Perdew, J. P.; Tao, J.; Staroverov, V. N.; Scuseria, G. E., *J. Chem. Phys.* **2004,** *120*, 6898-6911.
14. Becke, A. D., *J. Chem. Phys.* **1993,** *98*, 5648-5652.
15. Lee, C.; Yang, W.; Parr, R. G., *Phys. Rev. B* **1988,** *37*, 785-789.
16. Vosko, S. H.; Wilks, L.; Nusair, M., *Can. J. Phys.* **1980,** *58*, 1200-1211.
17. Stephens, P. J.; Devlin, F. J.; Chabalowski, C. F.; Frisch, M. J., *J. Phys. Chem.* **1994,** *98*, 11623-11627.
18. Pantazis, D. A.; Chen, X.-Y.; Landis, C. R.; Neese, F., *J. Chem. Theory Comput.* **2008,** *4*, 908-919.
19. Weigend, F.; Ahlrichs, R., *Phys. Chem. Chem. Phys.* **2005,** *7*, 3297-3305.
20. Römelt, M.; Ye, S.; Neese, F., *Inorg. Chem.* **2009,** *48*, 784-785.
21. Pápal, M.; Vankó, G., *J. Chem. Theory Comput.* **2013,** *9*, 5004-5020.
22. Sheldrick, G. M., *Acta Cryst.* **2008,** *A64*, 112-122.
23. Chen, C.; Lee, H.; Jordan, R. F., *Organometallics* **2010,** *29*, 5373-5381.